ORAL DISEASES

Oral Diseases (2012) 18, 568–574 doi:10.1111/j.1601-0825.2012.01909.x

www.wiley.com

ORIGINAL ARTICLE

Link between inflammation and aquaporin-5 distribution in submandibular gland in sjögren's syndrome?

MS Soyfoo[1,2], A Konno[3], N Bolaky[1], JS Oak[4], D Fruman[4], C Nicaise[5], M Takiguchi[6], C Delporte[1]

[1]*Laboratory of Biological Chemistry and Nutrition, Université Libre de Bruxelles, Brussels;* [2]*Department of Rheumatology, Erasme University Hospital, Brussels, Belgium;* [3]*Laboratory of Anatomy, Department of Veterinary Clinical Sciences, Graduate School of Veterinary Medicine, Hokkaido University, Sapporo, Japan;* [4]*Department of Molecular Biology and Biochemistry, Institute for Immunology, University of California, Irvine, CA, USA;* [5]*Laboratory of Histology, Neuroanatomy and Neuropathology, Université Libre de Bruxelles, Brussels, Belgium;* [6]*Laboratory of Veterinary Internal Medicine, Department of Veterinary Clinical Sciences, Graduate School of Veterinary Medicine, Hokkaido University, Sapporo, Japan*

OBJECTIVE: To determine whether a link exists between inflammation and aquaporin-5 distribution in submandibular glands from three animal models for Sjögren's syndrome: IQI/JIC, r1ΔT/r2n and non-obese diabetic mice.

METHODS: Mice of different ages were used. Inflammatory infiltrates were quantified using the focus score. Acinar aquaporin-5 subcellular distribution was determined by immunohistochemistry and quantified using labelling indices.

RESULTS: Minor inflammatory infiltrates were present in r1f/r2n mice. Massive inflammatory infiltrates and acinar destruction were observed in 24-week-old non-obese diabetic mice, 10-and 13-month-old IQI/JIC mice and some r1ΔT/r2n mice. Aquaporin-5 immunoreactivity was primarily apical in submandibular glands from 8- and 24-week-old Balb/C mice, 8-week-old non-obese diabetic mice, 2-, 4- and 7-month-old IQI/JIC mice and r1f/r2n mice. In contrast, decreased apical aquaporin-5 labelling index with concomitant increased apical-basolateral, apical-cytoplasmic and/or apical-basolateral-cytoplasmic aquaporin-5 labelling indices was observed in 24-week-old non-obese diabetic, 10- and 13-month-old IQI/JIC and r1ΔT/r2n mice with a focus score ≥ 1.

CONCLUSIONS: Altered aquaporin-5 distribution in submandibular acinar cells from IQI/JIC, non-obese diabetic and r1ΔT/r2n mice with a focus score ≥ 1 appears to be concomitant to the presence of inflammatory infiltrates and acinar destruction.

Oral Diseases (2012) **18**, 568–574

Correspondence: Prof Christine Delporte, PhD, Laboratory of Biological Chemistry and Nutrition, CP 611, Université Libre de Bruxelles, Route de Lennik 808, B-1070 Brussels, Belgium. Tel: +32 2 555 62 10, Fax: +32 2 555 62 30, E-mail: cdelport@ulb.ac.be
Received 19 October 2011; revised 21 December 2011; accepted 7 January 2012

Keywords: Sjögren's syndrome; exocrine glands; mice; autoimmune diseases; aquaporin-5

Introduction

Sjögren's syndrome (SS), a chronic inflammatory disease characterized by lymphocytic infiltration of salivary and lacrimal glands results in xerostomia and keratoconjunctivitis sicca, affects 0.1–0.6% of the population with a higher prevalence in middle-aged women (Fox, 2005; Trontzas and Andrianakos, 2005; Goransson *et al*, 2011). SS can be classified either as primary (pSS) or secondary (sSS) to other autoimmune diseases such as rheumatoid arthritis or systemic lupus erythematosus (Fox, 2005). The pathogenesis of SS is still not completely understood, and different mouse models of SS have been developed to unravel the mechanistic processes underlying the disease (Hansen *et al*, 2003). BAFF transgenic mice have enabled to demonstrate the pivotal role of B cells in the immune process while other mouse models have revealed different pathways leading to salivary gland destruction and ensuing sicca symptoms (van Blokland and Versnel, 2002; Groom *et al*, 2002; Soyfoo *et al*, 2007b). It is believed that sicca symptoms in SS results from a two-step process whereby lymphocytic infiltration of salivary glands occurs prior to gland destruction (Dawson *et al*, 2006a). However, a newer hypothesis stating the involvement of different pathways implying a wider array of pathophysiological mechanisms might be more relevant and account for the incomplete salivary gland destruction and the non-functionality of the remaining gland (Fox, 2005; Dawson *et al*, 2006a). New players intervening in the sicca process such as autoantibodies against muscarinic receptors and altered aquaporin-5 (AQP5) localization have been identified (Steinfeld *et al*, 2001; Tsubota *et al*, 2001; Naito *et al*, 2005; Dawson *et al*, 2006b).

AQP5 belongs to the aquaporin (AQPs) transmembrane protein family (Agre *et al*, 1995; Agre, 2004). Several AQPs, including AQP5, AQP1 and AQP8, have been reported to be expressed in salivary glands (Delporte and Steinfeld, 2006; Delporte, 2009). However, only AQP5 plays a pivotal role in saliva formation (Ma *et al*, 1999; Krane *et al*, 2001). Furthermore, alteration of AQPs expression and/or distribution occurs in secretory glands from patients with SS (Delporte, 2009). Concerning AQP5, altered localization has been shown in salivary glands and lacrimal glands from patients with SS, with reduced apical but increased basolateral localizations (Steinfeld *et al*, 2001; Tsubota *et al*, 2001). Similar AQP5 misdistribution was also observed in non-obese diabetic (NOD) mice, an appropriate animal model to study autoimmune exocrinopathy prevalent in SS (Konttinen *et al*, 2005; Soyfoo *et al*, 2007a). Indeed, with increasing age, NOD mice display histopathological modifications (inflammatory infiltrates and acinar cell destruction) and altered exocrine secretory gland function similar to those observed in patients with SS (Hu *et al*, 1992; Humphreys-Beher *et al*, 1994). Similar to NOD mice, the IQI/JIC mice have been recently described as a mouse model for primary SS. Indeed, these mice present lymphocytic infiltrates of exocrine and non-exocrine organs increasing in severity as they age (Takada *et al*, 2004). Besides, mice with T-cell-specific loss of class IA phosphoinositide 3-kinase function (r1ΔT/r2n mice) develop organ-specific autoimmunity that resembles the human SS disease (Oak *et al*, 2006). As a matter of fact, most of the r1ΔT/r2n mice aged 2–12 months develop corneal opacity and eye lesions, as well as cardinal signs of primary SS such as marked lymphocytic infiltration of the lacrimal glands, antinuclear antibodies in the serum and elevated titres of anti-SS-A antibody. The animal models described above represent unique tools to study the pathogenesis of SS.

The goal of our study was to investigate and compare the subcellular distribution of AQP5 in three different animal models for SS depicting different stages of SS: IQI/JIC mice, mice with phosphoinositide 3-kinase (PI3K)-deficient T cells (r1ΔT/r2n mice) and NOD mice.

Materials and methods

Animals

Female NOD and Balb/C (purchased at Harlan, Horst, the Netherlands) of 8 and 24 weeks of age were used. The origin of NOD mice has been previously described (Soyfoo *et al*, 2007a). As NOD mice also spontaneously develop autoimmune diabetes, mice were checked for glycosuria and only non-diabetic mice were included in the study. Maintenance of the animals and all experimental procedures were approved and performed in accordance with the Ethics Committees of the Catholic University (Leuven, Belgium).

The origin of IQI/JIC mice has been previously described (Takada *et al*, 2004). Female mice of 2, 4, 7, 10 and 13 months of age were used. All animal experiments were carried out with the approval of the Committee of Laboratory Animal Experimentation, Graduate School of Veterinary Medicine, Hokkaido University (Hokkaido, Japan).

Generation of r1f/r2n and r1ΔT/r2n mice has been previously described, and mice of 2–12 months of age were used (Luo *et al*, 2005; Oak *et al*, 2006). Male and female r1f/r2n (four females and one male) and r1ΔT/r2n (four females and three males) mice were used. Briefly, r1f/r2n mice are a strain possessing a floxed allele of *Pik3r1* (encoding the regulatory isoforms p85α, p55α and p50α) and a null allele of *Pik3r2* (encoding p85β). Crossing of r1f/r2n with the Lck-CRE transgenic mice generated the r1ΔT/r2n mouse strain, in which the function of PI3K is nullified in T cells. All animal procedures were approved by the institutional animal care and use committee of the University of California (Irvine, CA, USA).

Histology and immunohistochemistry

Immediately after removal, submandibular glands (SG) were fixed in 4% buffered formaldehyde, paraffin-embedded and sectioned (5 μm thick). Some salivary gland sections were stained with haematoxylin and eosin to visualize inflammatory infiltrates and acinar destruction. Quantification of inflammatory infiltrates in the submandibular glands was performed using the focus score (FS) (a FS of 1 corresponds to 50 lymphocytes per 4 mm^2 of tissue). The FS was determined following the examination of 10 fields of each salivary gland specimen. A FS of 0 or ≥1 was then assigned to each salivary gland examined. Immunostaining of AQP5 was performed as previously described using diaminobenzidine as chromogen (Soyfoo *et al*, 2007a). Negative control staining was performed in the absence of anti-AQP5 antibody or with anti-AQP5 antibody previously incubated with the immunizing peptide. Both negative controls showed the absence of specific staining.

Quantification of AQP5 labelling in submandibular glands

Ten salivary gland acini from 10 fields of the salivary gland specimen from six Balb/c (8 and 24 weeks of age), six NOD (8 and 24 weeks of age), six IQI-JIC (2, 4, 7, 10 and 13 months of age), five r1f/r2n, and seven r1ΔT/r2n mice were analysed in a blinded manner for acinar AQP5 subcellular localization. The acinar AQP5 immunoreactivity was classified into seven categories: (i) only at the apical membrane (A); (ii) at the apical membrane and the cytoplasm (AC); (iii) at the apical and basolateral membranes (AB); (iv) at the apical and basolateral membranes and the cytoplasm (ABC); (v) only at the basolateral membranes (B); (vi) at the basolateral membranes and the cytoplasm (BC); and (vii) only in the cytoplasm (C). The labelling index (LI) describes the percentage of acinar cells classified into one of the seven categories. Therefore, the labelling index clearly indicates the localization pattern of the AQP5 staining, and not the staining intensity.

Statistical analysis

Data are expressed as the mean ± s.e.m. Data were statistically analysed using ANOVA analysis with

Bonferroni multiple comparison post *t*-tests or unpaired *t*-test followed by a Bonferroni correction. All statistical analyses were carried out using GraphPad InStat version 5.0 (GraphPad Software, San Diego, CA, USA).

Results

Histological characteristics of submandibular glands from Balb/C, NOD, IQI/JIC, r1f/r2n and r1ΔT/r2n mice

Normal histological characteristics, that is, absence of lymphocytic infiltration and acini destruction, were observed in 8- and 24-week-old Balb/C mice, 8-week-old NOD mice, 2-, 4- and 7-month-old IQI/JIC mice. In r1f/r2n mouse models, minor lymphocytic infiltrates were observed and quantified as FS = 0. In contrast, extensive lymphocytic infiltration (FS ≥ 1) with destruction of acinar structures was observed in 24-week-old NOD mice, 10- and 13-month-old IQI/JIC mice and some r1ΔT/r2n mice (Figure 1). It is important to note that, in opposition to all the 24-week-old NOD and 10- and 13- month-old IQI/JIC mice presenting inflammatory infiltrates characterized by a FS ≥ 1, only three of the seven r1ΔT/r2n mice displayed inflammatory infiltrates characterized by a FS ≥ 1 while the four remaining presented a FS = 0. The quantification of the inflammatory infiltrates depicted by the FS is presented in Table 1 for all the mouse models studied.

Subcellular localization of AQP5 in submandibular glands

In all three mouse models depicting different stages of SS, acinar AQP5 localization was found to be apical (A), apical-basolateral (AB), apical-cytoplasmic (AC) and/or apical-basolateral-cytoplasmic (ABC), but never basolateral-cytoplasmic (BC), basolateral (B) or cytoplasmic (C) (Tables 2, 3 and 4). As the acinar AQP5 LI at the basolateral-cytoplasmic, basolateral or cytoplasmic were always equal to 0%, they were not indicated in Tables 2, 3 and 4.

In BALB/c mice, as well as in NOD and IQI/JIC mice displaying disease stages characterized by the absence of inflammation and acinar destruction, acinar AQP5 expression was primarily apical. Indeed, AQP5

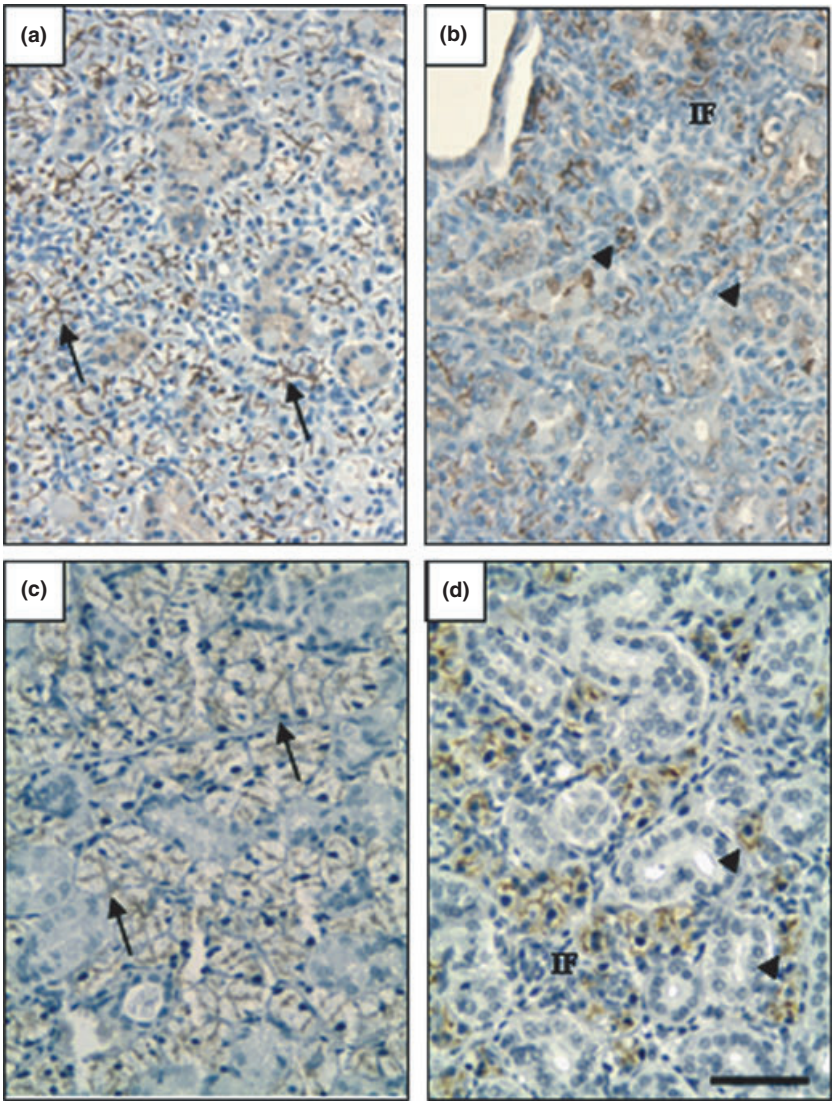

Figure 1 Localization of aquaporin-5 in submandibular glands from IQI/JIC mice, r1f/r2n and r1ΔT/r2n mice. Localization of AQP5 was determined by immunohistochemistry, as described in Materials and methods, in (**a**) 7-month-old IQI/JIC mice; (**b**) 10-month-old IQI/JIC mice; (**c**) r1f/r2n mice and (**d**) r1ΔT/r2n mice. Images are representative of immunohistochemical staining performed on salivary gland sections from six IQI/JIC mice of different age groups, five r1f/r2n mice with FS = 0 and three r1ΔT/r2n mice with FS ≥ 1. Bar scale represents 100 μm. Arrows show apical AQP5 staining, arrows heads show altered AQP5 staining. IF indicates the presence of inflammatory infiltrates

was mainly localized at the apical membrane in SG from 8- and 24-week-old BALB/c mice, 8-week-old NOD mice, and 2-, 4- and 7-month-old IQI/JIC mice (Tables 2 and 3). In NOD and IQI/JIC mice displaying disease stages characterized by inflammatory infiltrates and acinar cell destruction, the localization of AQP5 expression was modified. Indeed, compared with 8- and 24-week-old BALB/c and 8-week-old NOD mice, 24-week-old NOD mice had significant reduced acinar AQP5 LI at the apical membrane (A) with concomitant increased AQP5 LI at the apical and basolateral membranes (AB), the apical membrane and cytoplasm (AC), and the apical and basolateral membranes and cytoplasm (ABC) (Table 2). Compared with 2-, 4- and 7-month-old IQI/JIC mice, 10- and 13-month-old IQI/JIC mice displayed significant reduced acinar AQP5 LI at the apical membrane (A), with concomitant significantly increased AQP5 LI at the apical membrane and cytoplasm (AC), and at the apical and basolateral membranes and cytoplasm (ABC) (Table 3, Figure 1a,b).

Compared with r1f/r2n mice, used as negative control, r1ΔT/r2n mice taken with no distinction of FS exhibited no significant modification of AQP5 LI at all the seven possibilities of AQP5 distribution (Table 4). Nevertheless, r1ΔT/r2n mice appeared to be quite heterogeneous in terms of salivary gland inflammation: three mice of seven were characterized by a FS ≥ 1, while the four remaining mice were characterized by a FS = 0. Consequently, we further analysed AQP5 LI in

Table 1 Inflammatory focus score in submandibular glands from the different animal models

Mouse model	*Number of mice with a FS ≥ 1*
Balb/C	
8 weeks	0/6
24 weeks	0/6
NOD	
8 weeks	0/6
24 weeks	6/6
IQI/JIC	
2 months	0/6
4 months	0/6
7 months	0/6
10 months	6/6
13 months	6/6
r1f/r2n	0/5
r1ΔT/r2n	3/7

Quantification of inflammatory infiltrates in the submandibular glands was performed using the focus score (FS) (a FS of 1 corresponds to 50 lymphocytes per 4 mm^2 of tissue). The FS was determined as described in Materials and methods. A FS of 0 or ≥ 1 was assigned to each salivary gland examined.

Table 2 AQP5 labelling indices in submandibular glands from BALB/C and NOD mice

	LI A, %	*LI AB, %*	*LI AC, %*	*LI ABC, %*
8wBALB/C	89.2 ± 0.8	10.8 ± 0.8	0.0 ± 0.0	0.0 ± 0.0
8wNOD	86.1 ± 1.9	13.9 ± 1.9	0.0 ± 0.0	0.0 ± 0.0
24wBALB/C	91.3 ± 1.1	8.7 ± 1.1	0.0 ± 0.0	0.0 ± 0.0
24wNOD	15.8 ± 2.7$^{*\#\ddagger}$	35.6 ± 3.3$^{*\#\ddagger}$	21.8 ± 2.7$^{*\#\ddagger}$	27.2 ± 2.1$^{*\#\ddagger}$

Aquaporin-5 immunoreactivity was primarily apical in 8- and 24-week-old Balb/c and 8-week-old NOD mice. In 24-week-old NOD mice, aquaporin-5 A LI decreased, while AB LI, AC LI and ABC LI increased. Labelling indices of aquaporin-5 staining were determined as described in Materials and methods. Labelling indices were classified into categories: (i) only at the apical membrane (LI A); (ii) at the apical and basolateral membranes (LI AB); (iii) at the apical membrane and the cytoplasm (LI AC) and (iv) at the apical and basolateral membranes and the cytoplasm (LI ABC). The labelling index (LI) describes the percentage of acinar cells classified into one of the categories. The data are expressed as the LI ± s.e.m. of $n = 6$. Statistical analysis was performed using ANOVA analysis with Bonferroni multiple comparison post *t*-tests.
$^{*}P < 0.001$ compared with 8-week-old BALB/C; $^{\#}P < 0.001$ compared with 8-week-old NOD mice; $^{\ddagger}P < 0.001$ compared with 24-week-old BALB/C mice.

Table 3 AQP5 labelling indices in submandibular glands from IQI/JIC mice

	LI A, %	*LI AB, %*	*LI AC, %*	*LI ABC, %*
2mIQI/JIC	84.0 ± 1.9	16.0 ± 1.9	0.0 ± 0.0	0.0 ± 0.0
4mIQI/JIC	86.7 ± 2.0	13.3 ± 2.0	0.0 ± 0.0	0.0 ± 0.0
7mIQI/JIC	89.1 ± 1.6	10.9 ± 1.6	0.0 ± 0.0	0.0 ± 0.0
10mIQI/JIC	13.1 ± 0.9§*†	15.8 ± 2.4	41.8 ± 5.5§*†	28.9 ± 3.3§*†
13mIQI/JIC	23.6 ± 5.6§*†	12.0 ± 2.5	41.1 ± 4.1§*†	24.1 ± 4.1§*†

In 2-, 4- and 7-month-old IQI/JIC mice, aquaporin-5 distribution was primarily apical. In 10- and 13-month-old IQI/JIC mice, aquaporin-5 A LI decreased, while AC LI and ABC LI increased. Labelling indices of aquaporin-5 staining were determined as described in Materials and methods. Labelling indices were classified into categories: (i) only at the apical membrane (LI A); (ii) at the apical and basolateral membranes (LI AB); (iii) at the apical membrane and the cytoplasm (LI AC) and (iv) at the apical and basolateral membranes and the cytoplasm (LI ABC). The labelling index (LI) describes the percentage of acinar cells classified into one of the categories. The data are expressed as the LI ± s.e.m. of $n = 6$. Statistical analysis was performed using ANOVA analysis with Bonferroni multiple comparison post *t*-tests.
$^{\S}P < 0.001$ compared with 2-month-old IQI/Jic mice; $^{*}P < 0.001$ compared with 4-month-old IQI/Jic mice; $^{\dagger}P < 0.001$ compared with 7-month-old IQI/Jic mice.

Table 4 AQP5 labelling indices in submandibular glands from r1f/r2n and r1ΔT/r2n mice

	LI A, %	*LI AB, %*	*LI AC, %*	*LI ABC, %*
r1f/r2n (FS = 0; *n* = 5)	90.2 ± 2.1	9.0 ± 1.9	0.8 ± 0.8	0.0 ± 0.0
r1ΔT/r2n (*n* = 7)	42.2 ± 18.6	4.4 ± 1.6	27.6 ± 1.78	25.8 ± 17.0
r1ΔT/r2n (FS ≥ 1; *n* = 3)	4.1 ± 4.1*	2.3 ± 2.3	33.4 ± 33.4	60.2 ± 30.6
r1ΔT/r2n (FS = 0; *n* = 4)	70.8 ± 23.7	5.9 ± 2.1	23.3 ± 23.3	0.0 ± 0.0

In r1f/r2n and r1ΔT/r2n with FS = 0, aquaporin-5 distribution was primarily apical. In contrast, aquaporin-5 A LI was decreased in r1ΔT/r2n with FS ≥ 1. Labelling indices of aquaporin-5 staining were determined as described in Materials and methods. Labelling indices were classified into categories: (i) only at the apical membrane (LI AA); (ii) at the apical and basolateral membranes (LI AB); (iii) at the apical membrane and the cytoplasm (LI AC) and (iv) at the apical and basolateral membranes and the cytoplasm (LI ABC). The labelling index (LI) describes the percentage of acinar cells classified into one of the categories. Statistical analysis was performed using unpaired *t*-test followed by Bonferroni correction. The labelling index (LI) describes the percentage of acinar cells classified into one of the seven categories. The data are expressed as the LI ± s.e.m.
*$P < 0.05$ as compared to r1f/r2n mice. FS, focus score.

the SG from the two subgroups of r1ΔT/r2n mice presenting a FS ≥ 1 or a FS = 0. In the 3 r1ΔT/r2n mice displaying a FS ≥ 1, there was a significant decrease of AQP5 LI at the apical membrane (A) as compared to r1f/r2n mice (Table 4, Figure 1). In the four r1ΔT/r2n mice displaying a FS = 0, no significant modification of AQP5 LIs was detected compared with r1f/r2n mice (Table 4, Figure 1c,d).

Discussion

In the present study, we show that acinar AQP5 subcellular distribution in SG from three different mouse models for SS is altered and could be linked to inflammatory infiltrates. These observations support previous work on the abnormal subcellular distribution of AQP5 in salivary and lacrimal glands from pSS patients and mice (Steinfeld *et al*, 2001; Tsubota *et al*, 2001; Konttinen *et al*, 2005; Soyfoo *et al*, 2007a). As such, the abnormal distribution of AQP5 in the SG from mice models for SS could explain the defective salivary secretion characterizing SS, or result from pathological mechanisms occurring in SS. The second hypothesis was made following observations showing altered AQP5 distribution in SG, and not parotid, from NOD mice of 24 weeks of age, and the presence of lymphocytic infiltrates only in SG (Soyfoo *et al*, 2007a). To further assess the possible link between inflammation and altered AQP5 distribution, the subcellular localization of AQP5 was studied in relation to the presence of inflammatory infiltrates in three animal models for SS: NOD mice (used as a positive mice model for SS in this study), IQI/JIC mice and r1ΔT/r2n mice. Despite distinct molecular processes triggering SS in each animal model, the three animal models for SS have been shown to present extensive lymphocytic infiltration of salivary glands and lacrimal gland as well as acinar destruction, two major characteristics of SS (Oak *et al*, 2006; Soyfoo *et al*, 2007b).

To determine the labelling index of AQP5 in acini from SG, we used a fairly simple quantification method, which has the advantages to be less fastidious than computer-assisted quantification of immunohistochemical labelling or laser scanning confocal imaging, for example (Konttinen *et al*, 2005; Soyfoo *et al*, 2007a). This method is based on assigning acinar AQP5 labelling to a subcellular localization based on a matrix with seven possibilities of labelling localization: apical, apical-basolateral, apical-cytoplasmic, apical-basolateral-cytoplasmic, basolateral, basolateral-cytoplasmic or cytoplasmic localizations. Besides, to validate our method to quantify AQP5 labelling, AQP5 LI was first determined in SG from NOD mice that were previously shown to present AQP5 misdistribution (Konttinen *et al*, 2005; Soyfoo *et al*, 2007a). Our data were qualitatively similar to those obtained with computer-assisted quantification of immunohistochemical AQP5 labelling or laser scanning confocal imaging of AQP5 labelling in NOD mice and BALB/C mice (negative control) (Konttinen *et al*, 2005; Soyfoo *et al*, 2007a). Indeed, decreased apical AQP5 LI with concomitant increased apical-basolateral, apical-cytoplasmic and apical-basolateral-cytoplasmic AQP5 LI were observed in 24-week-old NOD, compared with 8-week-old NOD mice and 8- and 24-week-old BALB/C mice characterized by an AQP5 labelling being primarily apical and also apical-basolateral. Therefore, our quantification method was subsequently applied to study AQP5 subcellular localization in the two other animal models for SS: IQI/JIC and r1ΔT/r2n mice.

In SG acinar cells from 2-, 4-, 7-month-old IQI/JIC mice and r1f/r2n mice, AQP5 immunoreactivity was primarily apical and also apical-basolateral. In contrast, decreased apical AQP5 LI were observed in 10- and 13-month-old IQI/JIC mice and in r1ΔT/r2n mice displaying inflammatory infiltrates (FS ≥ 1). Concomitant increased apical-cytoplasmic and apical-basolateral-cytoplasmic AQP5 LI were observed in 10- and 13-month-old IQI/JIC mice.

In SG from control mice, AQP5 was expressed at both the apical and the basolateral membranes of acinar cells. The apical localization (Ma *et al*, 1999; Konttinen *et al*, 2005; Nandula *et al*, 2007) as well as the basolateral localization (Matsuzaki *et al*, 2006; Larsen *et al*, 2011) of AQP5 has been reported in mouse salivary glands. While the apical localization of AQP5 appears to be in agreement with its involvement in saliva secretion (Ma *et al*, 1999), AQP5 located at the basolateral membrane was suggested to act as

osmosensor regulating paracellular fluid movement (Murakami *et al*, 2006).

Under normal conditions, intracellular vesicles expressing AQP5 translocate to the apical membrane following muscarinic and adrenergic stimulation (Ishikawa *et al*, 2004, 2005). In all three mouse models for SS investigated, there was a shift in AQP5 distribution from the apical to the basolateral membrane, and intracellular vesicles. This AQP5 misdistribution could result from pathophysiological mechanisms occurring in SS. Under diseased conditions, AQP5 trafficking may be altered and intracellular vesicles expressing AQP5 may not be able to translocate to the apical membrane and therefore accumulate in the cytoplasmic compartment. Several mechanisms could be responsible for this alteration. First, defective activation of muscarinic M3 receptor could account for aberrant translocation of AQP5. Whether the abnormal distribution of AQP5 is linked to the presence of autoantibodies to M3 receptor (Naito *et al*, 2005) is an interesting question that still remains to be addressed in the mouse models for SS used in the present study. Second, altered expression of proteins involved in the regulation of AQP5, such as prolactin-inducible protein (Ohashi *et al*, 2008), could also account for AQP5 misdistribution. Third, inflammation may play a role in AQP5 altered distribution as impaired TGFß signalling has been shown to lead to an inflammatory disorder resembling Sjögren's syndrome and to a non-polarized and substantial intracellular localization of AQP5 (Nandula *et al*, 2007). Fourth, a defect in transcytosis may also account for altered AQP5 localization. In epithelial cells, plasma membrane proteins are sent to the correct surface through two pathways (Mostov *et al*, 1992; Song *et al*, 1994). The first pathway allows newly made proteins to be transported to the trans-Golgi network where they are packaged into vesicles that deliver them to the correct membrane surface. The second pathway delivers proteins to one membrane surface, usually the basolateral membrane, and proceeds to the endocytosis and the transcytosis of the proteins via vesicles to the apical membrane (Mostov *et al*, 1992). Physiologically, transcytosis of AQP5 proteins might also account for its basolateral localization in salivary glands from control animals.

Functionally, abnormal AQP5 distribution in acinar cells could account in part for the decreased saliva flow. However, in NOD mice, the moderate decrease in saliva flow rate did not match the extent of altered AQP5 distribution in acinar cells (Soyfoo *et al*, 2007a). Method of saliva collection, compensation of altered AQP5 distribution by increased AQP5 expression and reduced ability of water to permeate properly localized AQP5 might account for this discrepancy (Soyfoo *et al*, 2007a).

Inflammatory infiltrates and acinar destruction seemed to be concomitant to the observed AQP5 misdistribution in SG from the animal models for SS. Indeed, inflammatory infiltrates and acinar destruction were observed in SG displaying altered AQP5 labelling (24-week-old NOD mice, 10- and 13-month-old IQI/JIC mice and r1ΔT/r2n mice with a FS ≥ 1), but not in SG displaying primarily AQP5 expression at the apical membrane and also at the apical-basolateral membranes (8- and 24-week-old BALB/C mice, 8-week-old NOD mice, 2-, 4-, 7-month-old IQI/JIC mice, r1f/r2n mice and r1ΔT/r2n mice with a FS = 0). Parotid glands from NOD mice display no inflammatory infiltrates and normal apical AQP5 distribution (Soyfoo *et al*, 2007a). Changes in AQP5 localization could therefore be temporally linked to the inflammatory mechanisms (and to the extent of lymphocytic infiltrates) underscoring the pathogenesis of SS. Interactions between different pro-inflammatory cytokines, which have been advocated to contribute to the inflammatory infiltrates in the salivary glands of patients with SS (Manoussakis *et al*, 2007; Nandula *et al*, 2007; Bikker *et al*, 2010), may play a role in the modification of AQP5 localization.

The observations made in the present study indirectly support the involvement of inflammatory infiltrates as potential culprits in the aberrant localization of AQP5 in salivary glands from SS mouse models, without excluding that other mechanisms might also contribute to defective AQP5 trafficking.

In conclusion, altered AQP5 distribution was observed in acinar cells from SG from three mouse models for SS: IQI/JIC, NOD mice and r1ΔT/r2n mice with a FS ≥ 1. AQP5 misdistribution appears to be concomitant to the presence of inflammatory infiltrates and acinar destruction. Further studies will be required to precisely define the molecular events involved in AQP5 misdistribution and this in relation to the temporal progression of the inflammatory processes and the disease.

Acknowledgements

This work was supported by grant 3.4502.09 from the Fund for Medical Scientific Research (FNRS, Belgium). We are very grateful to Prof. C. Mathieu for sharing the NOD mice model.

Author contributions

M.S.S. designed and performed experiments, acquired and analysed data and drafted manuscript; A.K. performed experiments and revised manuscript; N.B. performed experiments; J.S.O. performed experiments, acquired data; N.B. performed experiments; D.F. performed experiments, acquired data and revised manuscript; C.N. analysed data and revised manuscript; M.T. performed experiments and revised manuscript; C.D. designed experiments, analysed data and revised manuscript.

Conflicts of interest

The authors declare no conflicts of interest and no financial disclosures.

References

Agre P (2004). Aquaporin water channels (Nobel Lecture). *Angew Chem Int Ed Engl* **43:** 4278–4290.

Agre P, Brown D, Nielsen S (1995). Aquaporin water channels: unanswered questions and unresolved controversies. *Curr Opin Cell Biol* **7:** 472–483.

Bikker A, van Woerkom JM, Kruize AA *et al* (2010). Increased expression of interleukin-7 in labial salivary glands of patients with primary Sjogren's syndrome correlates with increased inflammation. *Arthritis Rheum* **62:** 969–977.

van Blokland SC, Versnel MA (2002). Pathogenesis of Sjogren's syndrome: characteristics of different mouse models for autoimmune exocrinopathy. *Clin Immunol* **103:** 111–124.

Dawson LJ, Fox PC, Smith PM (2006a). Sjogrens syndrome: the non-apoptotic model of glandular hypofunction. *Rheumatology (Oxford)* **45:** 792–798.

Dawson LJ, Stanbury J, Venn N, Hasdimir B, Rogers SN, Smith PM (2006b). Antimuscarinic antibodies in primary Sjogren's syndrome reversibly inhibit the mechanism of fluid secretion by human submandibular salivary acinar cells. *Arthritis Rheum* **54:** 1165–1173.

Delporte C (2009). Aquaporins in secretory glands and their role in Sjogren's syndrome. *Handb Exp Pharmacol* **18:** 5–201.

Delporte C, Steinfeld S (2006). Distribution and roles of aquaporins in salivary glands. *Biochim Biophys Acta* **1758:** 1061–1070.

Fox RI (2005). Sjogren's syndrome. *Lancet* **366:** 321–331.

Goransson LG, Haldorsen K, Brun JG *et al* (2011). The point prevalence of clinically relevant primary Sjogren's syndrome in two Norwegian counties. *Scand J Rheumatol* **40:** 221–224.

Groom J, Kalled SL, Cutler AH *et al* (2002). Association of BAFF/BLyS overexpression and altered B cell differentiation with Sjogren's syndrome. *J Clin Invest* **109:** 59–68.

Hansen A, Lipsky PE, Dorner T (2003). New concepts in the pathogenesis of Sjogren syndrome: many questions, fewer answers. *Curr Opin Rheumatol* **15:** 563–570.

Hu Y, Nakagawa Y, Purushotham KR, Humphreys-Beher MG (1992). Functional changes in salivary glands of autoimmune disease-prone NOD mice. *Am J Physiol* **263:** E607–E614.

Humphreys-Beher MG, Hu Y, Nakagawa Y, Wang PL, Purushotham KR (1994). Utilization of the non-obese diabetic (NOD) mouse as an animal model for the study of secondary Sjogren's syndrome. *Adv Exp Med Biol* **350:** 631–636.

Ishikawa Y, Inoue N, Zhenfang Y, Nakae Y (2004). Molecular mechanisms and drug development in aquaporin water channel diseases: the translocation of aquaporin-5 from lipid rafts to the apical plasma membranes of parotid glands of normal rats and the impairment of it in diabetic or aged rats. *J Pharmacol Sci* **96:** 271–275.

Ishikawa Y, Yuan Z, Inoue N *et al* (2005). Identification of AQP5 in lipid rafts and its translocation to apical membranes by activation of M3 mAChRs in interlobular ducts of rat parotid gland. *Am J Physiol* **289:** C1303–C1311.

Konttinen YT, Tensing EK, Laine M, Porola P, Tornwall J, Hukkanen M (2005). Abnormal distribution of aquaporin-5 in salivary glands in the NOD mouse model for Sjogren's syndrome. *J Rheumatol* **32:** 1071–1075.

Krane CM, Melvin JE, Nguyen HV *et al* (2001). Salivary acinar cells from aquaporin 5-deficient mice have decreased membrane water permeability and altered cell volume regulation. *J Biol Chem* **276:** 23413–23420.

Larsen HS, Aure MH, Peters SB, Larsen M, Messelt EB, Kanli Galtung H (2011). Localization of AQP5 during development of the mouse submandibular salivary gland. *J Mol Histol* **42:** 71–81.

Luo J, McMullen JR, Sobkiw CL *et al* (2005). Class IA phosphoinositide 3-kinase regulates heart size and physiological cardiac hypertrophy. *Mol Cell Biol* **25:** 9491–9502.

Ma T, Song Y, Gillespie A, Carlson EJ, Epstein CJ, Verkman AS (1999). Defective secretion of saliva in transgenic mice lacking aquaporin-5 water channels. *J Biol Chem* **274:** 20071–20074.

Manoussakis MN, Boiu S, Korkolopoulou P *et al* (2007). Rates of infiltration by macrophages and dendritic cells and expression of interleukin-18 and interleukin-12 in the chronic inflammatory lesions of Sjogren's syndrome: correlation with certain features of immune hyperactivity and factors associated with high risk of lymphoma development. *Arthritis Rheum* **56:** 3977–3988.

Matsuzaki T, Ablimit A, Suzuki T, Aoki T, Hagiwara H, Takata K (2006). Changes of aquaporin 5-distribution during release and reaccumulation of secretory granules in isoproterenol-treated mouse parotid gland. *J Electron Microsc* **55:** 183–189.

Mostov K, Apodaca G, Aroeti B, Okamoto C (1992). Plasma membrane protein sorting in polarized epithelial cells. *J Cell Biol* **116:** 577–583.

Murakami M, Murdiastuti K, Hosoi K, Hill AE (2006). AQP and the control of fluid transport in a salivary gland. *J Membr Biol* **210:** 91–103.

Naito Y, Matsumoto I, Wakamatsu E *et al* (2005). Muscarinic acetylcholine receptor autoantibodies in patients with Sjogren's syndrome. *Ann Rheum Dis* **64:** 510–541.

Nandula SR, Amarnath S, Molinolo A *et al* (2007). Female mice are more susceptible to developing inflammatory disorders due to impaired transforming growth factor beta signaling in salivary glands. *Arthritis Rheum* **56:** 1798–1805.

Oak JS, Deane JA, Kharas MG *et al* (2006). Sjogren's syndrome-like disease in mice with T cells lacking class 1A phosphoinositide-3-kinase. *Proc Natl Acad Sci U S A* **103:** 16882–16887.

Ohashi Y, Tsuzaka K, Takeuchi T, Sasaki Y, Tsubota K. Altered distribution of aquaporin 5 and its C-terminal binding protein in the lacrimal glands of a mouse model for Sjögren's syndrome. *Curr Eye Res* **33:** 621–629.

Song W, Apodaca G, Mostov K (1994). Transcytosis of the polymeric immunoglobulin receptor is regulated in multiple intracellular compartments. *J Biol Chem* **269:** 29474–29480.

Soyfoo MS, De Vriese C, Debaix H *et al* (2007a). Modified aquaporin 5 expression and distribution in submandibular glands from NOD mice displaying autoimmune exocrinopathy. *Arthritis Rheum* **56:** 2566–2574.

Soyfoo MS, Steinfeld S, Delporte C (2007b). Usefulness of mouse models to study the pathogenesis of Sjogren's syndrome. *Oral Dis* **13:** 366–375.

Steinfeld S, Cogan E, King LS, Agre P, Kiss R, Delporte C (2001). Abnormal distribution of aquaporin-5 water channel protein in salivary glands from Sjogren's syndrome patients. *Lab Invest* **81:** 143–148.

Takada K, Takiguchi M, Konno A, Inaba M (2004). Spontaneous development of multiple glandular and extraglandular lesions in aged IQI/Jic mice: a model for primary Sjogren's syndrome. *Rheumatology (Oxford)* **43:** 858–862.

Trontzas PI, Andrianakos AA (2005). Sjogren's syndrome: a population based study of prevalence in Greece. The ESORDIG study. *Ann Rheum Dis* **64:** 1240–1241.

Tsubota K, Hirai S, King LS, Agre P, Ishida N (2001). Defective cellular trafficking of lacrimal gland aquaporin-5 in Sjogren's syndrome. *Lancet* **357:** 688–689.